

# Immunoglobulin G4-related disease complicated with vascular lesions: CT findings in 21 patients

Lin Qi\* 

Dingbiao Mao\* 

Li Xiao 

Xiu Jin 

Ming Li 

Yanqing Hua 

## PURPOSE

We aimed to analyze multislice computed tomography (MSCT) imaging features of vasculitis in immunoglobulin G4-related disease (IgG4-RD).

## METHODS

In this retrospective study, we diagnosed 21 definite or possible IgG4-RD patients (71.4% male; mean age, 52.1±4.5 years) with vasculitis by MSCT and pathologic examination. The clinical background, laboratory analysis, pathologic results, CT images, and response to therapy were assessed and analyzed.

## RESULTS

Under enhanced MSCT, 50 vasculitic lesions were identified and were divided into five types (types A–E) according to the CT findings on the basis of luminal changes. There were more vasculitic lesions observed below the diaphragm (n=30) than above it (n=20). Aneurysms and aneurysmal dilatation were more likely to be found in the aortaventralis (n=5), aortic arch (n=3) and iliac arteries (n=3). Most of the vascular lesions were characterized by wall thickening with a normal lumen (n=15) and slight stenosis (n=22). The affected vascular walls were all thickened between 4 and 18 mm. The walls of 19 patients (90.4%) were well circumscribed. The wall thickness of the aorta, including the aortaventralis and aortic arch, was more notable than that of the other vascular sites. Fourteen patients were followed up for 2–24 months. Wall thickness decreased in all cases. The average maximum thicknesses before and after therapy were 12.2±2.7 mm and 6.1±1.8 mm, which were significantly different ( $P < 0.001$ ). The lumens of two patients were found to be slightly enlarged, while those of the other cases were unchanged after therapy.

## CONCLUSION

IgG4-RD vascular lesions can be divided into five types, which are more likely to be present in the aorta and its main branches, and can rapidly diminish after steroid therapy. The lumen may be unchanged or slightly enlarged.

Immunoglobulin G4-related disease (IgG4-RD) is a systemic chronic inflammatory fibrotic disease, in which patients present with high serum IgG4 levels and IgG4-positive plasma cells that infiltrate target organs. IgG4-RD has recently come to be regarded as a new clinicopathologic entity (1). In IgG4-RD, dysfunction can be detected in many different organs, including the bile duct, central nervous system, lymph nodes, pancreas, liver, kidney, prostate, retroperitoneum, intestinal tract, breast, skin, and cardiovascular system (2). Cardiovascular involvement in IgG4-RD has not been fully elucidated and may present as inflammatory perivasculitis, coronary arteritis, and/or pericarditis (3).

Radiologic imaging and serologic examination of serum IgG4 levels are both critical elements in the final diagnosis of vasculitis in IgG4-RD patients. Autoimmune pancreatitis, for example, is highly suspected based on radiologic examination due to its characteristic results and is ultimately verified through serologic analysis of IgG4 levels. Thus, identifying the radiographic features of vasculitis in IgG4-RD is of great importance. Our aim in this retrospective study was to examine the role of imaging modalities, especially multislice computed tomography (MSCT), in the diagnosis and follow-up of this rare disease.

From the Departments of Radiology (L.Q., D.M., X.J., M.L. ✉ [minli77@163.com](mailto:minli77@163.com), Y.H.) and Pathology (L.X.), Huadong Hospital Fudan University, Shanghai, China.

\* Lin Qi and Dingbiao Mao contributed equally to this work.

Received 22 April 2018; revision requested 23 May 2018; last revision received 15 June 2018; accepted 24 June 2018.

DOI 10.5152/dir.2018.18174

You may cite this article as: Qi L, Mao D, Xiao L, Jin X, Li M, Hua Y. Immunoglobulin G4-related disease complicated with vascular lesions: CT findings in 21 patients. *Diagn Interv Radiol* 2019; 25: 42–49.

## Methods

### Study population and data collection

In this retrospective study, we diagnosed 21 patients with definite or possible IgG4-RD, accompanied by vascular disease according to MSCT and pathologic examination. The Institutional Review Board of our hospital approved the study (protocol number: 20170721), and written informed consent was obtained from all individuals. MSCT examinations were performed with a 64-slice MSCT scanner (Sensation 64, Siemens Medical Solutions). The scanning parameters were as follows: section thickness, 1 mm; tube voltage, 120 kVp; tube current, 300 mA. The arterial phase was obtained with a delay of between 30 s and 40 s after the administration of 90–120 mL of contrast medium at a rate of 3.5–4.5 mL/s. The venous phase was obtained with a delay of between 90 s and 120 s after the injection. The clinical background, laboratory analysis, pathologic examination, CT images, and response to therapy were assessed and analyzed. Among the 21 patients who were enrolled, 18 (85.7%) had pathologic examinations of vasculitis lesions or target organs, consisting of hematoxylin-eosin (H-E) and immunohistochemistry staining for IgG and IgG4. No obvious complications were found among the study patients during this period with respect to the use of anti-hypertensive and antidyslipidemic therapy, corticosteroids or immunosuppressive drugs. All 21 patients underwent CT angiography. Six underwent positron emission tomography/ computed tomography (PET/CT). The cardiovascular CT angiographic image datasets were analyzed using vessel analysis software. Two readers with more than 7 years of clinical experience in cardiovascular CT angiography performance and analysis independently evaluated the reconstructed images. When there was any

disagreement in the data analysis between the two readers, a consensus agreement was reached.

### Diagnostic criteria

The diagnostic criteria for IgG4-RD are as follows (4): 1) distinct changes in target organs; 2) a serum IgG4 concentration >135 mg/dL; and 3) lymphocytes and IgG4-positive plasma cell infiltration and fibrosis upon histopathologic examination, with a ratio of IgG4-positive/IgG-positive plasmacytes >40%, and >10% IgG4-positive plasmacytes/high-power field. For a definitive diagnosis of IgG4-RD, all three sets of criteria must be satisfied. Cases meeting only criteria 1 and 2 are diagnosed as possible IgG4-RD.

### Statistical analysis

Statistical analysis was performed using SPSS software (version 22.0; IBM Corp.). Data were expressed as mean±standard deviation. Wall thickness before and after steroid therapy were analyzed for differences using paired-samples t test. A *P* value <0.05 was considered statistically significant.

## Results

The clinical data of the 21 patients are

shown in Table 1. The mean age of the patients in the study was 52.1±4.5 years, and 71.4% of the patients were male. Eighteen individuals were given a definite diagnosis of vasculitis in IgG4-RD. Pathologic and immunohistochemical analyses were not performed in three of the patients. Coronary artery lesions were found upon PET/CT and coronary CT angiography in one of the patients, and IgG4 was also elevated in the serum of this patient. Two other patients exhibited characteristic imaging features of IgG4-RD in their organs without evidence of an associated inflammatory reaction. Therefore, these patients received a diagnosis of IgG4-RD. Obtaining samples from coronary arteries for histologic examination is often more difficult than obtaining samples from lesions in other organs. Therefore, imaging findings and serum biomarkers are useful for the diagnosis of IgG4-related periarteritis. However, histologic analysis of other vessels, such as the aorta, may be necessary for patients with chronic periaortitis, including inflammatory abdominal aortic aneurysms and retroperitoneal fibrosis, which are frequently similar in patients with IgG4-related and non-IgG4-related disease (5). These patients received prednisolone at an initial

**Table 1.** Baseline characteristics of the study patients

Characteristics	Values
Age (years), mean±SD	52.1±4.5
Male gender, n (%)	15 (71.4)
Body mass index (kg/m <sup>2</sup> ), mean±SD	25.2±3.5
Systolic BP (mmHg), mean±SD	126±16.7
Diastolic BP (mmHg), mean±SD	87.2±13.4
Hypertension, n (%)	6 (28.6)
Total cholesterol (mmol/dL), mean±SD	5.26±0.87
HDL (mmol/dL), mean±SD	1.38±0.33
LDL (mmol/dL), mean±SD	2.46±0.67
Triglycerides (mmol/dL), mean±SD	1.77±0.65
Diabetes, n (%)	4 (19%)
Dyslipidemia, n (%)	5 (23.8)
Current smoker, n (%)	6 (28.5)
CRP (mg/L), median (min–max)	3.34 (0.98–6.67)
Satisfaction for diagnostic criteria	19 (90.5)

SD, standard deviation; BP, blood pressure; HDL, high-density lipoprotein; LDL, low-density lipoprotein; CRP, c-reactive protein.

### Main points

- We present the role of imaging modalities especially computed tomographic angiography in diagnosis of IgG4-related disease (IgG4-RD).
- CT findings of vasculitis of IgG4-RD were divided into five types based on luminal changes.
- CT is also useful for follow-up of IgG4-related inflammatory lesions and evaluation of disease activity during and after steroid therapy for its noninvasive characteristics.

**Table 2.** Characteristics of perivascular infiltration and perivascular IgG4-related lesions in 21 cases

Case	Clinical symptom	Perivascular lesions	Type	Other organ infiltration	IgG (mg/dL)	IgG4 (mg/dL)	Diagnosis
1	Chest distress	Coronary artery	A-B	Autoimmune pancreatitis	1678	371	Definite
2	Chest pain	CA	C	None	1548	297	Suspected
3	Weight loss	CIA	E	Autoimmune pancreatitis	2170	455	Definite
4	None	AOAR, DAO	A-B	Autoimmune pancreatitis	2351	721	Definite
5	None	AOAR	B	None	1936	651	Definite
6	Jaundice	SPA, CA	B	Sclerosing cholangitis	1874	483	Definite
7	None	AA, CIA	A-B	Autoimmune pancreatitis, LNs	2920	1100	Definite
8	Back pain	AA, CIA	A-B	Retroperitoneal fibrosis	1768	368	Definite
9	Jaundice, back pain	AAO, AOAR	A-E	A renal lesion, sclerosing cholangitis	1690	351	Definite
10	Back pain	AOAR, CIA	A-B-D	Autoimmune pancreatitis	1895	278	Suspected
11	Lacrimation	AAO, AA	A-B-D	Intraorbital inflammation, LNs	1490	198	Definite
12	Diabetes	AA, CA	B-E	Autoimmune pancreatitis	2160	345	Definite
13	Back pain	AA, CIA	D-E	Paravertebral mass, LNs	1990	423	Definite
14	None	CIA	A-B-D	Intraorbital inflammation	2764	982	Definite
15	None	AA, IMA	A-B-D	Autoimmune pancreatitis	1580	255	Definite
16	None	AOAR, AAO	B-D	Autoimmune pancreatitis, LNs	3110	1312	Definite
17	Apocleisis	AA, SMA, CA, RA	A-B	Retroperitoneal fibrosis	1985	534	Suspected
18	Anuria	AA, SMA, CA	A-B	Retroperitoneal fibrosis	2258	433	Definite
19	None	CA	A	Autoimmune pancreatitis	1550	326	Definite
20	Back pain, Jaundice	AOAR, DAO, AA, CIA	A-B-E	Autoimmune pancreatitis, sclerosing cholangitis	1647	679	Definite
21	Back pain	PA, AA, CIA	A-B-E	Retroperitoneal fibrosis, sialadenitis, LNs	1447	552	Definite

Type A: periarteritis with normal caliber; it has the hallmark of a perivascular soft tissue mass surrounding the artery with normal caliber. Type B: periarteritis with mild luminal stenosis. Type C: Periarteritis with moderate luminal stenosis. Type D: aneurysmal dilatation with periarteritis; <50% of the expected normal diameter with wall thickening. Type E: aneurysm with periarteritis; >50% of the expected normal diameter with wall thickening.  
CA, celiac artery; CIA, common iliac artery; AOAR, aortic arch; DAO, descending aorta; SPA, splenic artery; AA, abdominal aorta; LN, lymph node; AAO, ascending aorta; IMA, inferior mesenteric artery; SMA, superior mesenteric artery; RA, renal artery; PA, pulmonary artery.

dose of 30 mg/day, which was gradually reduced to a maintenance dose of 5 mg/day based on the improvement of clinical findings and inflammatory manifestations.

Five types of vasculitic infiltration of IgG4-RD were found upon CT, based on luminal changes. Type A was periarteritis with a normal caliber, and it showed the hallmarks of a perivascular soft tissue mass surrounding the artery with a normal caliber. Type B indicated periarteritis with mild luminal stenosis (luminal stenosis <50%). Type C was periarteritis with moderate luminal stenosis (luminal stenosis 50%–70%). Type D was aneurysmal dilatation with periarteritis, where

<50% of the expected normal diameter is seen with wall thickening. Type E indicated aneurysm with periarteritis, where >50% of the expected normal diameter is seen with wall thickening.

Enhanced CT revealed 50 sites of perivascular lesions, which are listed in Table 2. They were located in the thoracic aorta (n=14, 28%), including the ascending aorta (n=2, 4%), aortic arch (n=7, 14%), descending aorta (n=5, 10%), coronary artery (n=2, 4%), pulmonary artery (n=1, 2%), left subclavian artery (n=1, 2%), left common carotid artery (n=1, 2%), brachiocephalic trunk (n=1, 2%), aortaventrals (n=11, 22%), celiac trunk

(n=5, 10%), splenic artery (n=1, 2%), iliac artery (n=9, 18%), renal artery (n=1, 2%) IMA (n=1, 2%), and SMA (n=2, 4%).

Periarteritis with a normal caliber (type A) was found in 15 arteries, including the aortic arch (n=2), ascending aorta (n=2), descending aorta (n=2), pulmonary artery (n=1), aortaventrals (n=3), celiac trunk (n=2), iliac artery (n=2), and SMA (n=1).

Twenty-two lesions were classified as type B, including lesions of the aortic arch (n=2), descending aorta (n=3), coronary artery (n=1), splenic artery (n=1), left subclavian artery (n=1), left common carotid artery (n=1), brachiocephalic trunk (n=1), aortaventrals

**Table 3.** Types of perivascular lesions

Vasculitis	n (%)	Type A+B	Type D+E	Max wall thickness (mm) mean±SD	Atherosclerotic change n (%)
Aortaventralis	11 (22)	6	5	12±4.6	5 (45)
Iliac artery	9 (22)	6	3	9±3.7	2 (22)
Aorta arch	7 (14)	4	3	13±3.5	4 (57)
Descending aorta	5 (10)	5	0	8±3.1	2 (40)
Celiac trunk	5 (10)	5	0	5±2.7	1 (20)
Coronary artery	2 (4)	1	0	14.5	0
SMA	2 (4)	2	0	9.1	0
IMA	1 (2)	1	0	6	0
Pulmonary artery	1 (2)	1	0	5	0
Renal artery	1 (2)	1	0	6	0
Splenic artery	1 (2)	1	0	6	0

SD, standard deviation; SMA, superior mesenteric artery; IMA, inferior mesenteric artery.

**Table 4.** Wall and luminal change after therapy

Case	Max wall thickness before therapy (mm)	Max wall thickness change after therapy (mm)	Vessel luminal change after therapy
1	14	8	Unchanged
2	13	4	Slight enlargement
3	9	5	Unchanged
4	12	6	Unchanged
5	16	10	Unchanged
8	10	6	Unchanged
9	15	6	Unchanged
10	15	9	Slight enlargement
11	9	4	Unchanged
12	15	7	Unchanged
16	11	6	Unchanged
18	8	4	Unchanged
19	12	5	Unchanged

(n=3), celiac trunk (n=3), iliac artery (n=4), renal artery (n=1), and IMA (n=1).

One case showed type C vascular lesions in the coronary artery without infiltration of any other organ, and these lesions were reclassified as type B lesions after one month of prednisolone treatment.

Type D lesions were found in 6 arteries, including the aortaventralis (n=2), iliac ar-

tery (n=3), and SMA (n=1), with a diameter of 26±5 mm and wall thickness of 17±6 mm. Type E lesions were found in 6 arteries, including the aortaventralis (n=3) and aortic arch (n=3), with a diameter of 55±14 mm and wall thickness of 25±12 mm. Thrombosis was found in two aortaventralis aneurysms.

There were more perivascular lesions observed in vessels under the diaphragm

(n=30) than above the diaphragm (n=20). Aneurysms tended to be found in the aorta, including in the aortaventralis (n=3) and the aortic arch (n=3). Most vascular lesions showed wall thickening with a normal lumen (n=15) and slight stenosis (n=22). The average maximum thickness of pseudotumors around the arterial and/or aortic walls was 12 mm (4–18 mm). Nineteen of the lesions (90.4%) were well circumscribed. The wall thickness of the aorta, including that of the aortaventralis and the aortic arch, was more notable than at other vascular sites (Table 3). Aneurysms and aneurysmal dilatation were more likely to be found in the aortaventralis (n=5), aortic arch (n=3), and iliac artery (n=3).

The involvement of other organs in the 21 patients included autoimmune pancreatitis (n=10) (Fig. 1), LNs (n=12), sialadenitis (n=3), retroperitoneal fibrosis (n=4), renal lesions (n=1), sclerosing cholangitis (n=3), intraorbital inflammation (n=1), and a paravertebral mass (n=1).

All patients underwent arterial phase contrast-enhanced CT, and the pseudotumors around arterial and/or aortic walls showed nonenhancement. Fifteen of the patients (71%) underwent late-phase contrast-enhanced CT and showed slight, homogeneous enhancement.

Six patients underwent PET/CT (Cases 1, 7, 8, 13, 16, and 18). All of the patients were found to exhibit enhanced uptake of 18F-fluorodeoxyglucose (FDG) in the lymph nodes and perivascular masses in the aorta and the coronary arteries, consistent with the CT imaging findings.

Pathologic examinations were performed in 18 patients (Cases 1, 3–9, 11–16, and 18–21). Pathologic diagnosis of IgG4-related disease was achieved using the specimens obtained from wall tissue exhibiting periaortitis or perivasculitis (surgical resection or needle biopsies in Cases 1, 5, 6, 8, 14, 17, and 18) (Fig. 2), pancreas (needle biopsies in Cases 3, 4, 7, 10, 12, 15, 19, and 20), salivary gland (needle biopsy in Case 21), paravertebral mass (needle biopsy in Case 13), renal mass (surgical resection in Case 9), and LNs (surgical resection in Cases 11 and 16). The original resected specimens or specimens from patients who underwent biopsy were available and were reviewed by a pathologist with 11 years of experience. The diagnosis was based on pathologic features such as diffuse lymphoplasmacytic infiltration, irregular fibrosis, obliterative phlebitis, occasional eosinophilic infiltration, infiltration of numerous IgG4-positive plasma cells, and a high ratio of IgG4/IgG-positive plasma cells (>30%) (6–8).

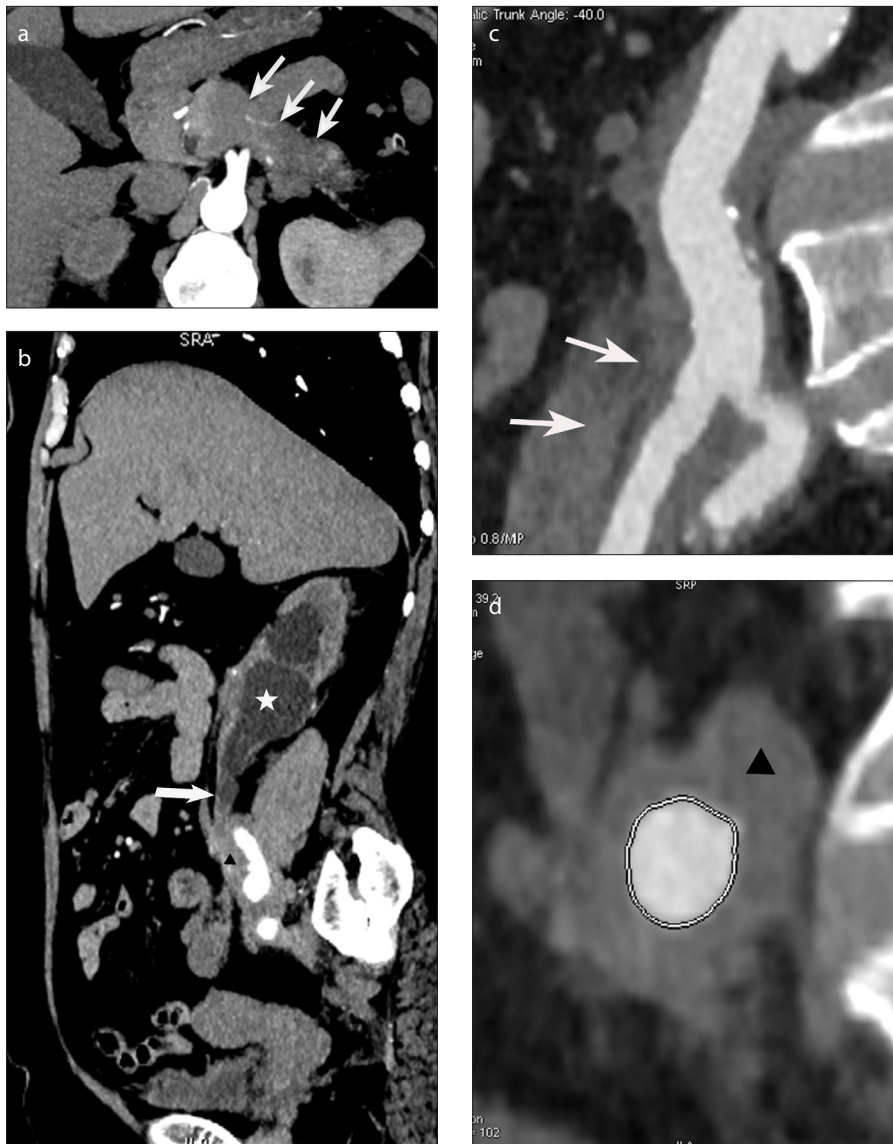


**Figure 1.** a–d. Contrast-enhanced CT scans of IgG4-RD with vascular lesions in a 68-year-old man (Case 3). Axial image (a) shows the diffuse swelling of pancreas (arrows). Oblique image (b) demonstrates encasement of inferior segment of the right ureter (black arrowhead), leading to hydronephrosis (white arrow) and hydroureter (star). Reconstructed image (c) shows the moderate thickening of right iliac artery wall (white arrow) associated with slight luminal dilatation (type E). Oblique image (d) shows that the border of the perivascular lesion is smooth and the lesion stretches to its branches (black arrowhead).

Fourteen patients were followed up over 2–24 months (the median term was 10 months, in Cases 1–5, 8–10, 11–12, 16, 18, 19, and 20). Wall thickness decreased in all cases. The average maximum thickness before and after therapy were  $12.2 \pm 2.7$  mm and  $6.1 \pm 1.8$  mm, which were significantly different ( $P < 0.001$ ). Case 20 manifested only slight thickening of the celiac trunk wall. After 2 months of corticosteroid treatment, perivasculitis disappeared from the celiac trunk wall, and the serum IgG-4 level was normal. Case 10 was found to exhibit slight enlargement of the aortic arch aneurysm after corticosteroid

treatment for 8 months. The aortic and/or arterial wall thickness in the other 12 patients was considerably decreased due to steroid therapy, but the diameter of the involved vessels was unchanged except in Case 2, in which the type of coronary stenosis changed to type B. The diameter of the aneurysms and/or aneurysmal dilatation was not changed in Cases 4, 8, 11, and 12 (Table 4).

## Discussion

We identified IgG4-related disease with periaortitis or perivasculitis in 21 patients

who were diagnosed based on immunohistochemical findings or radiologic examinations, similar to a study by Dai Inoue et al. (9). Most of the individuals with IgG4-RD vascular disease were adult males, and the serum IgG4 concentration was the most characteristic serologic parameter. Vascular lesions were characterized by wall thickening, homogeneous enhancement in the late phase of contrast-enhanced CT, distinct and clear borders, and luminal changes.

In the present study, however, the CT findings were divided into five types based on luminal changes. Most of the vascular lesions exhibited wall thickening with a normal lumen (30%, type A) and slight stenosis (44%, type B). Aneurysms were more likely to be found in the aorta, for example, in the aortaventrals and the aortic arch. Aneurysms (type E) and aneurysmal dilatation (type D) tended to be found in the aortaventrals, aortic arch, and iliac artery. The type of coronary lesions in Case 2 changed from type C to type B after 2 months of treatment, so the five types could be considered different stages of vascular infiltration.

In our study, 90% of the patients with IgG4-RD perivasculitis showed involvement of other organs, a rate that was much higher than previously reported (9). This result was likely due to the fact that it is difficult to diagnose IgG4-RD perivasculitis without characteristic clinical implications of other organs such as autoimmune pancreatitis. Radiologic features, increased serum IgG4 concentrations, and characteristic involvement of other organs are speculated to be important clues that are sufficient for the diagnosis of IgG4-RD perivasculitis; however, pathologic examination is usually absent or difficult to perform. Nevertheless, pathologic examination is necessary for precise differentiation from retroperitoneal fibrosis reduced for other reasons.

Inflammatory abdominal aortic aneurysm (IAAA) is one of the most common lesions observed in IgG4-RD, which is estimated to account for 5% of surgical abdominal aortic aneurysms and 50% of total IAAs (10–13). IgG4-related aneurysms are reported in medium- to large-sized arteries. In our study, aneurysms and aneurysmal dilatation showed a tendency to be found in the aortaventrals, aortic arch, and the iliac artery. Pathologically, most of the IgG4-related aneurysms and aortitis cases showed IgG4-positive cells and eosinophil infiltration in the adventitia, but some cases also showed infiltration in the

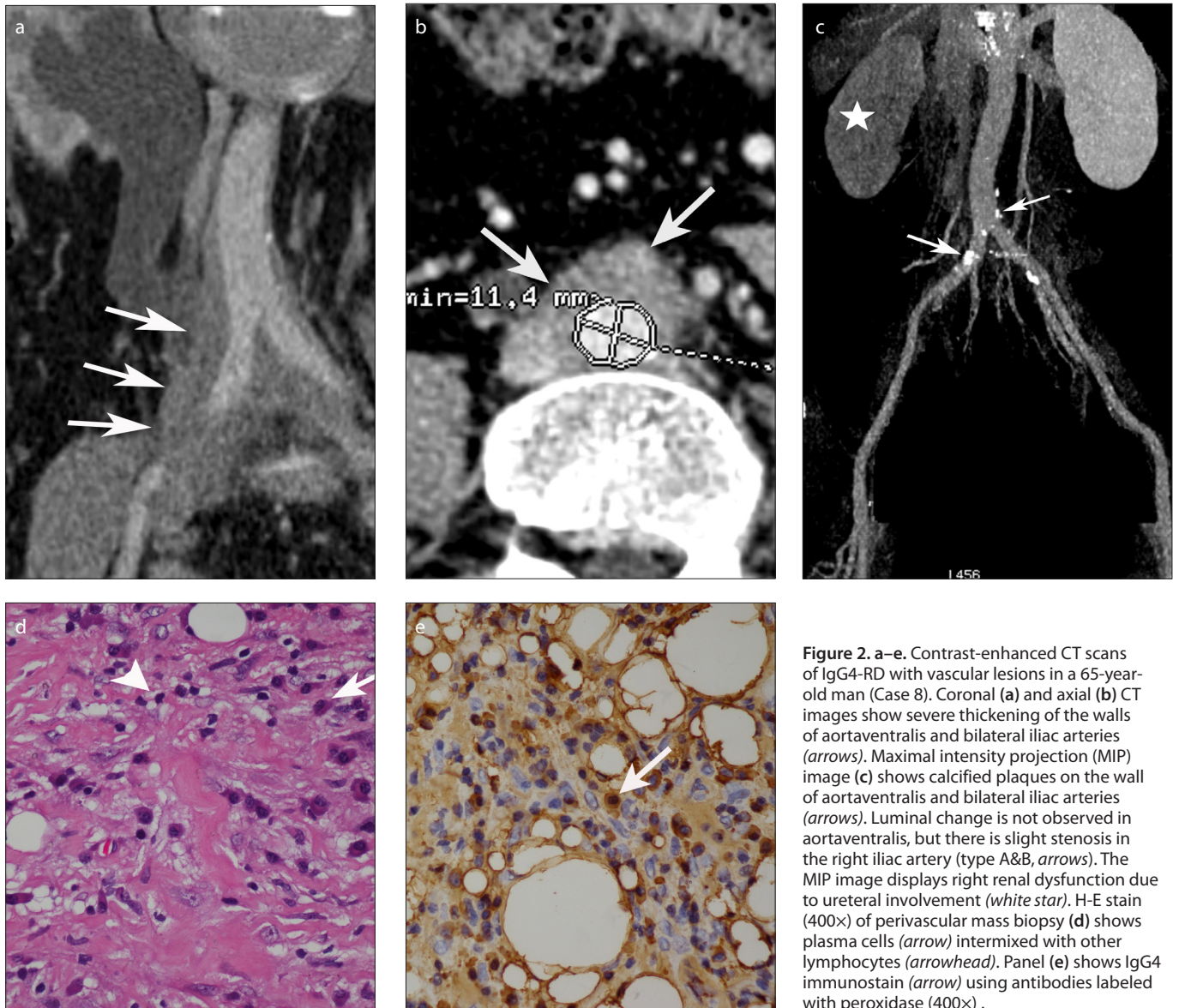


**Figure 2. a–e.** Contrast-enhanced CT scans of IgG4-RD with vascular lesions in a 65-year-old man (Case 8). Coronal (a) and axial (b) CT images show severe thickening of the walls of aortaventrals and bilateral iliac arteries (arrows). Maximal intensity projection (MIP) image (c) shows calcified plaques on the wall of aortaventrals and bilateral iliac arteries (arrows). Luminal change is not observed in aortaventrals, but there is slight stenosis in the right iliac artery (type A&B, arrows). The MIP image displays right renal dysfunction due to ureteral involvement (white star). H-E stain (400 $\times$ ) of perivascular mass biopsy (d) shows plasma cells (arrow) intermixed with other lymphocytes (arrowhead). Panel (e) shows IgG4 immunostain (arrow) using antibodies labeled with peroxidase (400 $\times$ ).

intima in addition to the adventitia, leading to aneurysm formation. T helper 2 (TH2) cells have been reported to cause apoptosis of vascular smooth muscle cells, which may give rise to an aneurysm (14). Proximal large arteries exhibit plentiful smooth muscle cells to tolerate high blood pressure, which may be the reason that aneurysms are prone to primarily develop in the large arteries.

Steroid therapy is now well recognized as the first-line therapy for IgG4-RD. Steroids can reduce inflammation by suppressing lymphocyte activation to prevent further development of inflammatory lesions, including aortitis/arteritis and aneurysms (15). However, the effects of steroid therapy on aneurysms are unclear. Some studies have indicated that steroid therapy cannot

shrink the size of an already-developed aneurysm (16). During the follow-up period in our research, the diameters of aneurysms and aneurysmal dilatation did not change, but wall thickness decreased considerably. In contrast, according to other studies reported in the literature (17–19), reduction of the periarterial pseudotumor and thinning of the arterial wall during corticosteroid therapy may increase the risk of aneurysmal rupture. Given these findings, regular follow-up during corticosteroid therapy is of great significance. Surgical treatment may be chosen in cases of a ruptured aneurysm, which is much more difficult to perform than for an atherosclerotic aneurysm due to the adhesion of intraabdominal organs (20).

Several reports have indicated that

IgG4-RD may be associated with certain coronary artery diseases, such as coronary pseudotumors, wall calcification, aneurysms, and intimal thickening (21). In our study, Case 1 was found to exhibit autoimmune pancreatitis and a focal soft tissue mass around the middle segment of the right coronary artery. Case 2 had diffuse pseudotumors around the proximal left anterior descending branch and along the whole course of the right coronary artery and left circumflex, without infiltration of other organs (Fig. 3). There was a myocardial bridge in the middle left anterior descending branch, and the segment of the myocardial bridging-mural coronary artery (MB-MCA) and the distal were normal. We believe that perhaps the MB-MCA is a

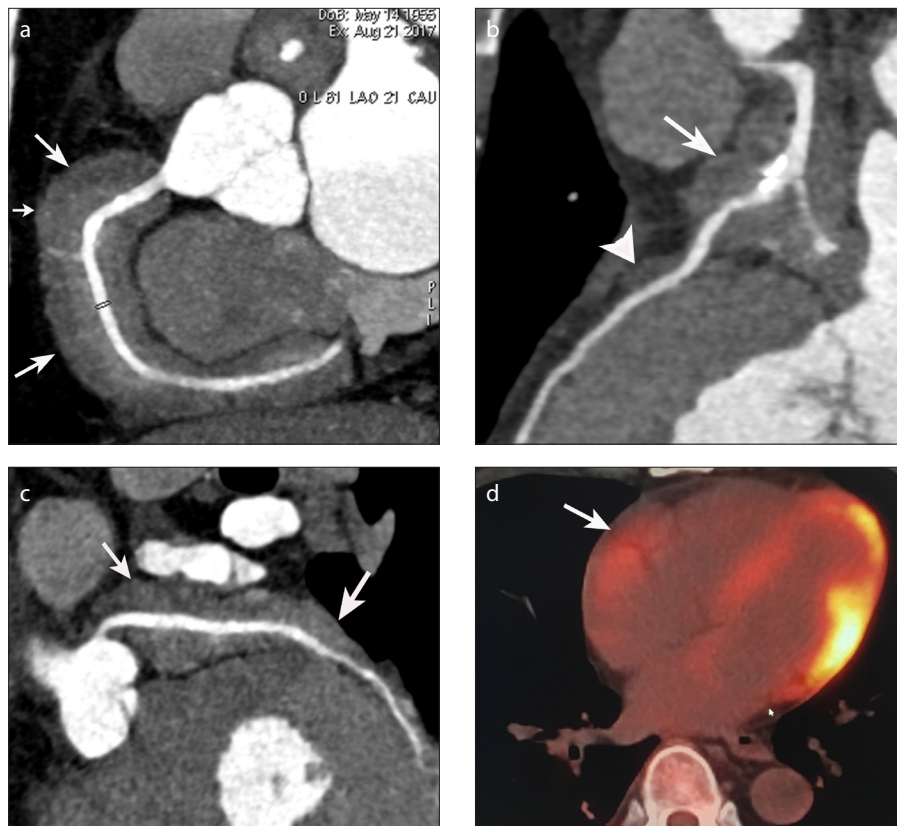


**Figure 3.** a–d. Case 1, a 69-year-old man with coronary artery infiltration. Curved multiplanar reconstruction images (a–c) show diffuse pseudotumors around the whole course of RCA (a), proximal LAD (b), and LCX (c, arrows). There is a myocardial bridge in the middle left anterior descending branch (b, arrowhead). The segment of myocardial bridging-mural coronary artery of LAD and the distal are normal. Slight stenosis is visible in proximal LAD while the lumens of RCA and LCX are normal (Type A and B). PET-CT (d) shows intermediate grade uptake in the region of RCA (arrow).

protective factor in the case of IgG4-related coronary artery disease.

A wide distribution of vascular lesions is another important feature of IgG4-related vasculitis. Moreover, more lesions were observed in the vessels below rather than above the diaphragm in this study, and the lesions were prone to occur in large- and mid-sized vessels. Infiltration of other organs was found in most of the IgG4-RD patients (90%) at the same time. In our retrospective study, we failed to observe all of the suspected arteries, such as the coronary arteries and part of the aorta. Thus, we could not obtain comprehensive diagnostic information for all the patients. These results reveal that IgG4-RD is a multiorgan and systemic disease, and once IgG4-RD is diagnosed in one organ, CT angiography of large- and mid-sized vessels should be performed to exclude the possibility of vascular infiltration.

A limitation of this retrospective study was the short follow-up time, which meant that we failed to observe a response to ster-

oid therapy. Another limitation was that pathologic diagnosis was not performed in all of the cases due to the difficulty of obtaining specimens around the arteries.

In conclusion, contrast-enhanced CT may allow the identification of more cases of IgG4-related vasculitis by chance; because patients may not present with any symptoms corresponding to this disease or for the evaluation of disease activity during and after steroid therapy due to its noninvasive characteristics (23).

#### Financial disclosure

This study was supported by the Research Program of Shanghai Hospital Development Center SHDC22015025 (Ming Li); the National Key Research and Development Program of China 2017YFC0112800 (Peijun Wang), 2017YFC0112905 (Ming Li); the Medical Imaging Key Program of Wise Information Technology of 120, Health Commission of Shanghai 2018ZHYL0103 (Ming Li); Cardiology Group of Key Specialty Construction

Program of Pudong Health Bureau of Shanghai (PW-Zxq2017-01); General Research Projects of Health Bureau of Shanghai 2017 (201740199).

#### Conflict of interest disclosure

The authors declared no conflicts of interest.

#### References

1. Kamisawa T, Zen Y, Pillai S, Stone JH. IgG4-related disease. *Lancet* 2015; 385:1460–1471. [\[CrossRef\]](#)
2. Kamisawa T, Funata N, Hayashi Y, et al. A new clinicopathological entity of IgG4-related autoimmune disease. *J Gastroenterol* 2003; 38:982–984. [\[CrossRef\]](#)
3. Mavrogeni S, Markousis-Mavrogenis G, Kolovou G. IgG4-related cardiovascular disease. The emerging role of cardiovascular imaging. *Eur J Radiol* 2017; 86:169–175. [\[CrossRef\]](#)
4. Umehara H, Okazaki K, Masaki Y, et al. Comprehensive diagnostic criteria for IgG4-related disease (IgG4-RD), 2011. *Mod Rheumatol* 2012; 22:21–30. [\[CrossRef\]](#)
5. Qian Q, Kashani KB, Miller DV. Ruptured abdominal aortic aneurysm related to IgG4 periaortitis. *NJEM* 2009; 361:1121–1123. [\[CrossRef\]](#)
6. Kasashima S, Zen Y, Kawashima A, et al. Inflammatory abdominal aortic aneurysm: close relationship to IgG4-related periaortitis. *Am J Surg Pathol* 2008; 32:197–204. [\[CrossRef\]](#)
7. Kitagawa S, Zen Y, Harada K, et al. Abundant IgG4-positive plasma cell infiltration characterizes chronic sclerosing sialadenitis (Kuttner's tumor). *Am J Surg Pathol* 2005; 29:783–791. [\[CrossRef\]](#)
8. Cornell LD, Chicano SL, Deshpande V, et al. Pseudotumors due to IgG4 immune-complex tubulointerstitial nephritis associated with autoimmune pancreatocentric disease. *Am J Surg Pathol* 2007; 31:1586–1597. [\[CrossRef\]](#)
9. Inoue D, Zen Y, Abo H, et al. Immunoglobulin G4-related periaortitis and periarteritis: CT findings in 17 patients. *Radiology* 2011; 261:625–633. [\[CrossRef\]](#)
10. Ishida M, Hotta M, Kushima R, Asai T, Okabe H. IgG4-related inflammatory aneurysm of the aortic arch. *Pathol Int* 2009; 59:269–273. [\[CrossRef\]](#)
11. Ikutomi M, Matsumura T, Iwata H, et al. Giant tumorous lesions (correction of legions) surrounding the right coronary artery associated with immunoglobulin G4-related systemic disease. *Cardiology* 2011; 120:22–26. [\[CrossRef\]](#)
12. Kasashima S, Zen Y. IgG4-related inflammatory abdominal aortic aneurysm. *Curr Opin Rheumatol* 2011; 23:18–23. [\[CrossRef\]](#)
13. Kasashima S, Zen Y, Kawashima A, et al. A clinicopathologic study of immunoglobulin G4-related sclerosing disease of the thoracic aorta. *J Vasc Surg* 2010; 52:1587–1595. [\[CrossRef\]](#)
14. Henderson EL, Geng YJ, Sukhova GK, Whittemore AD, Knox J, Libby P. Death of smooth muscle cells and expression of mediators of apoptosis by T lymphocytes in human abdominal aortic aneurysms. *Circulation* 1999; 99:96–104. [\[CrossRef\]](#)
15. Cha MJ, Chong S, Kim YS, Park B, Seo JH, Lee ES. Immunoglobulin G4-related periaortitis involving the aortic arch mimicking a mediastinal tumor. *Ann Thorac Surg* 2017; 103:e267–e270. [\[CrossRef\]](#)

16. Tajima M, Hiroi Y, Takazawa Y, et al. Immunoglobulin G4-related multiple systemic aneurysms and splenic aneurysm rupture during steroid therapy. *Hum Pathol* 2014; 45:175–179. [\[CrossRef\]](#)
17. Davis FM, Rateri DL, Daugherty A. Abdominal aortic aneurysm: novel mechanisms and therapies. *Curr Opin Cardiol* 2015; 30:566–573. [\[CrossRef\]](#)
18. Matsumoto Y, Kasashima S, Kawashima A, et al. A case of multiple immunoglobulin G4-related periarteritis: a tumorous lesion of the coronary artery and abdominal aortic aneurysm. *Hum Pathol* 2008 ;39:975–980. [\[CrossRef\]](#)
19. Puchner S, Bucek RA, Loewe C, et al. Endovascular repair of inflammatory aortic aneurysms: long-term results. *AJR Am J Roentgenol* 2006;186:1144–1147. [\[CrossRef\]](#)
20. Trinidad-Hernandez M, Duncan AA. Contained ruptured paravisceral aortic aneurysm related to immunoglobulin G4 aortitis. *Ann Vasc Surg* 2012; 26:108 e1–4.
21. Ishizaka N. IgG4-related disease underlying the pathogenesis of coronary artery disease. *Clin Chim Acta*; 2013; 415:220–225. [\[CrossRef\]](#)
22. Fujinaga Y, Kadoya M, Kawa S, et al. Characteristic findings in images of extra-pancreatic lesions associated with autoimmune pancreatitis. *Eur J Radiol* 2010; 76:228–238. [\[CrossRef\]](#)
23. Ebe H, Tsuboi H, Hagiya C, et al. Clinical features of patients with IgG4-related disease complicated with perivascular lesions. *Mod Rheumatol* 2015; 25:105–109. [\[CrossRef\]](#)